Hindawi
International Journal of Aerospace Engineering
Volume 2018, Article ID 4854656, 10 pages
https://doi.org/10.1155/2018/4854656

Research Article

Experimental Investigation on the Feasibility of Using Spring-Loaded Pogo Pin as a Holding and Release Mechanism for CubeSat's Deployable Solar Panels

Tae-Yong Park,[1] **Su-Hyeon Kim**,[1] **Hongrae Kim**,[2] **and Hyun-Ung Oh**[1]

[1]*Space Technology Synthesis Laboratory, Department of Aerospace Engineering, Chosun University, Gwangju, Republic of Korea*
[2]*Soletop Co. Ltd., 409 Expo-ro, Yuseong-gu, Daejeon, Republic of Korea*

Correspondence should be addressed to Hyun-Ung Oh; ohu129@chosun.ac.kr

Received 23 February 2018; Accepted 19 July 2018; Published 9 September 2018

Academic Editor: James D. Biggs

A spring-loaded pogo pin as a holding and release mechanism of solar panels for cube satellite applications is proposed which functions as an electrical interface, a separation spring, and a status switch. The proposed mechanism has many advantages, including an increased loading capability, negligible induced shock level, synchronous release of multiple panels, and handling simplicity during integration. A demonstration model of the mechanism was fabricated and functionally tested under various test conditions such as different input voltages, different numbers of tightened nylon wires, and different temperatures (ranging from −40°C to 70°C).

1. Introduction

A cube satellite (CubeSat) is a type of cube-shaped pico-class miniaturized satellite with a volume of 10 cm^3 and a mass less than 1.33 kg with respect to a standard size of one unit (1 U) [1]. Recently, a CubeSat had been used for increasingly complex missions [2–7], and its functionality in an extremely small package leads to numerous mechanisms and deployable structures that are necessary to achieve challenging mission-related functions. Deployable structures, including solar arrays, antennas, sensors, and other appendages, are stowed for launch and are released and deployed in orbit for successful mission execution. The deployable appendages require holding and release mechanisms that provide adequate strength and stiffness to survive in the launch environment and release functions to allow the deployment of these appendages in orbit.

Recently, various holding and release mechanisms (HRMs) were developed for the separation of the deployable structures for CubeSat applications. Pyrotechnic devices are extensively used in the aerospace engineering field and particularly in commercial satellite separation. They typically induce increased levels of shock responses owing to the sudden transient release of strain energy. The high-frequency pyroshock sometimes causes malfunctions of electrical components or critical damage to the brittle components of on-board equipment [8]. The issue of the increased shock induced by the activation of the pyrotechnic device constitutes an even more critical challenge for pico-class satellites because the main components are in closer physical proximity from the source of shock in CubeSats compared with larger satellites owing to the extremely low sizes and volume limitations of the CubeSats.

In order to reduce the shock caused by pyrotechnic devices, several types of nonexplosive separation devices using shape memory alloy (SMA) [9, 10] actuators have been developed and used in actual space missions [11–13]. The advantages of the nonexplosive SMA actuators include lower shock responses, higher load capability, and reusability for additional cycles after a simple reset. However, even though the shock level is low, the use of these devices may still be associated with a few limitations with respect to CubeSat usage owing to their high cost and because they do not satisfy typical pico-satellite requirements, such as low weight, small

size, and the capability to generate relatively small shocks. The increased cost of these devices makes it impractical to use them in CubeSat applications.

A nichrome burn wire cutting method was extensively used for the release of mechanical constraints on the deployable appendages of a CubeSat owing to its simplicity and low cost. The mechanical constraint was released by cutting the nylon cable triggered by a nichrome burn wire. Nakaya et al. [14] developed a cable-cutting separation mechanism for cube satellite separation from a launcher. The four jaws of the mechanism that held the cube satellite during launch were tightened by a nylon cable, and this was then cut by heating a nichrome wire. Thurn et al. [15] developed a burn wire release mechanism to release the tether deployment system. This mechanism utilized a compression spring system to apply a force and stroke to the nichrome burn wire to ensure a safer release. They conducted functional performance tests in vacuum, and the test results indicated a shorter cut time of the mechanism under vacuum when compared to that in air. A turnstile antenna developed by GomSpace [16] consisted of four monopole antennas with nearly omnidirectional coverage. All four antenna beams were individually fixed by a nylon cable and released by the activation of burn resistors. Oh and Lee [17] developed a segmented nut-type HRM with various advantages, including an increased load capacity and negligible shock. The nut segment constructed using a nylon cable winding was released by cutting the nylon cable by using the nichrome burn wire. The effectiveness of the design was verified based on a functionality test and static load tests under qualification temperature limits on a demonstration model of the mechanism. Lee et al. [18] also developed a new version of the hinge driving separation nut-type HRM, and this was simpler than that proposed by Oh et al. [17]. It did not require an outer housing with Velcro fasteners to avoid interference between the released nut and the constraint bolt immediately after separation. The mechanism's main payload has been verified based on the Cube Laboratory for Space Technology Experimental Project (STEP Cube Lab) mission [19].

In this study, a new version of a nichrome burn wire-triggered HRM using a spring-loaded pogo pin is proposed and investigated, and this is developed for the separation device of solar panels for various CubeSat applications. A pogo pin [20] is a device that is extensively used in electronics to establish a temporary connection between two printed circuit boards (PCBs). This constitutes an extremely attractive function for the application of separation devices because it functions as an electrical interface to provide power, a separation spring to initiate reaction force, and a status switch to determine a deployment status of the solar panel. The advantages of the mechanism proposed in the study include increased loading capability in the in-plane and out-of-plane directions of solar panels, low-shock levels, synchronous release of multiple panels, and handling simplicity during the tightening process of the nylon wire. The release function of the mechanism was verified by performing a separation test under various test conditions. These test results demonstrated that the proposed mechanism verified the feasibility of using pogo pins as a holding and release mechanism of solar panels for CubeSat applications in accordance with the proposed design.

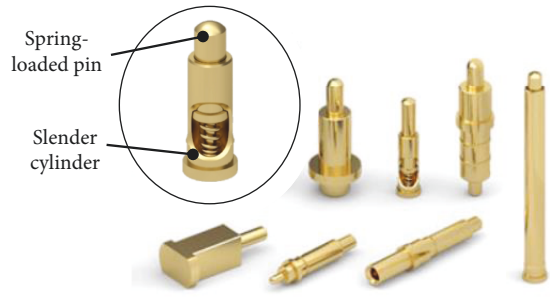

Figure 1: Example of a spring-loaded pogo pin [21].

2. Holding and Release Mechanism Using Spring-Loaded Pogo Pins

2.1. Spring-Loaded Pogo Pins. Figure 1 shows an example of spring-loaded pogo pins [21] arranged in a dense array on two circuit boards used in electronics to establish a temporary electrical connection. They are extensively used in automatic test equipment in the form of a bed of nails wherein they facilitate a rapid and reliable connection of the tested devices. They are also used to establish a more permanent connection. The pogo pin consists of a slender cylinder and spring-loaded pin. The sharp points at the end of the pogo pin form secure contacts between the two circuits induced by the restoration force of the spring-loaded pogo pin. They must be designed in an extremely careful manner to achieve increased reliability across many mating and demating cycles as well as high-fidelity transmission of the electrical signals [22].

With respect to the CubeSat applications, Oh et al. [23] proposed the use of pogo pins for the electrical connection between an MEMS solid propellant thruster array and its control circuit board, as shown in Figure 2. The design allows the thruster module to be easily mounted or dismounted from the fully integrated satellite without disassembling any satellite parts during testing and transportation to the launch site. The thruster module was developed to verify a main payload through the STEP Cube Lab mission [19]. The effectiveness of the design and reliable electrical contact using the pogo pins was verified based on launch vibration and a thermal vacuum test at the qualification level.

2.2. Design Description of HRM with Pogo Pins. The design driver in the study involves developing a new version of burn wire release-type HRM for a deployable solar panel of a CubeSat with high loading capability along in-plane and out-of-plane directions of the solar panel, synchronous release of multiple panels, and handling simplicity during the tightening process of the nylon wire. An extremely important feature of the HRM proposed in this study involves using spring-loaded pogo pins as an electrical power interface to provide power to burn wire triggering resistor. Additionally, they also used them as a separation spring

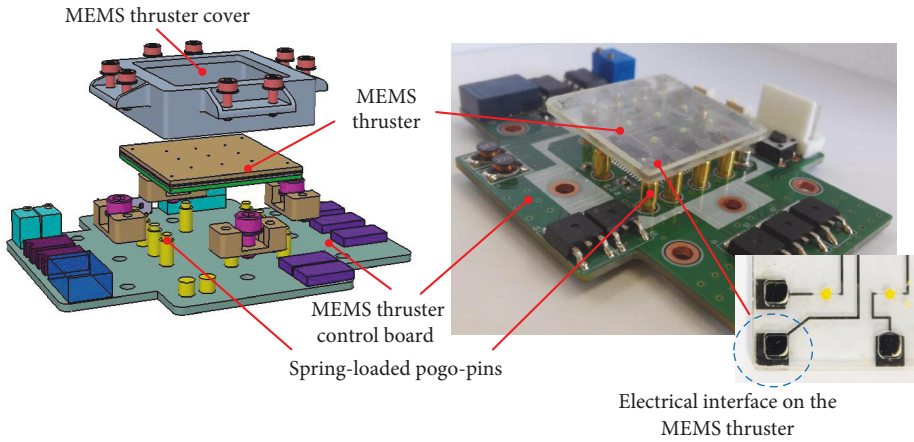

Figure 2: MEMS-based solid propellant thruster and its control board with spring-loaded pogo pin [22].

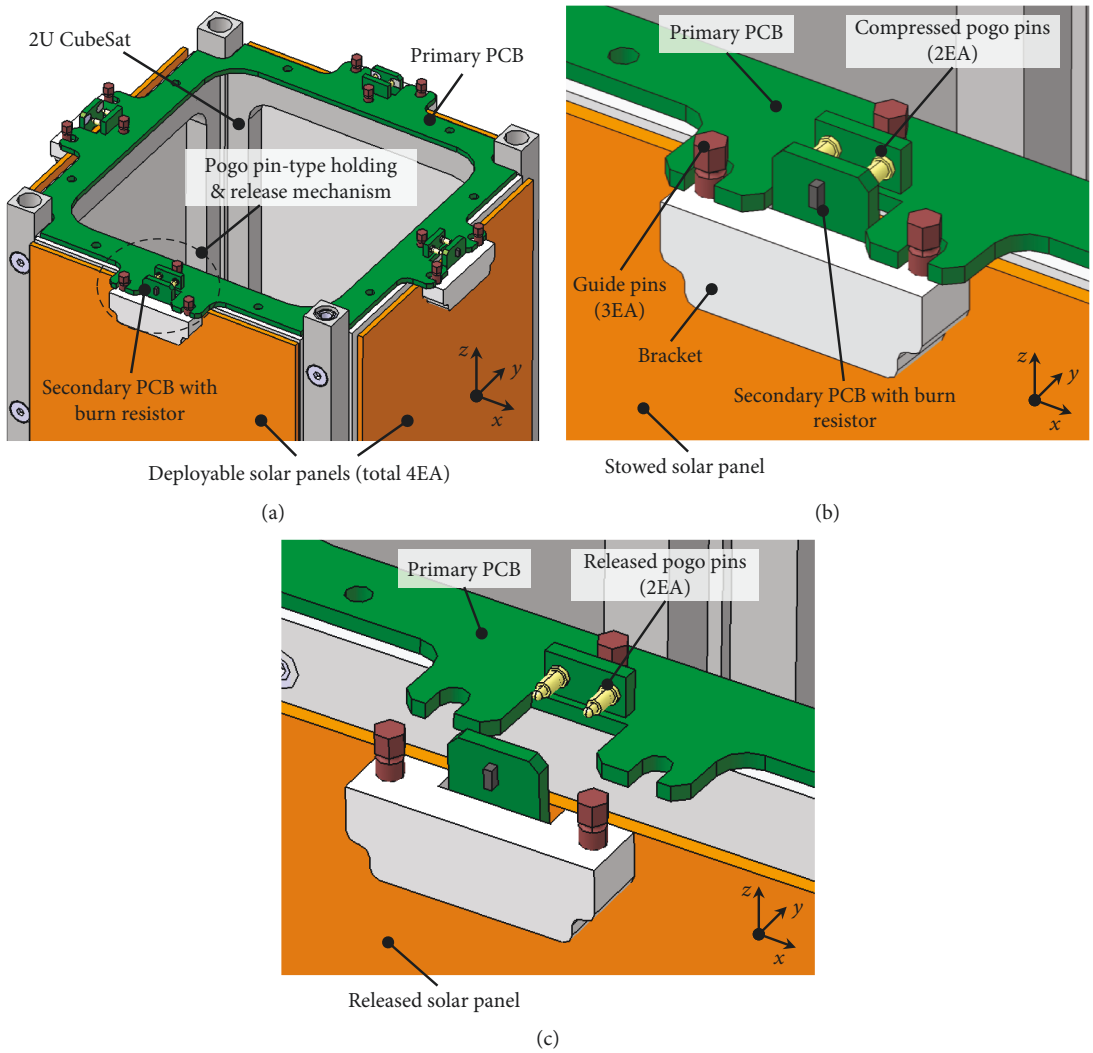

Figure 3: Configuration of a pogo pin-type holding and release mechanism proposed in the study: (a) overall configuration, (b) holding state, and (c) release state.

to initiate a reaction force to the solar panel and status switch to determine deploy and stow statuses of the deployable panels.

Figure 3 shows the stowed and released configurations of the pogo pin-type HRM developed in the study. Figure 4 shows the demonstration model of the HRM.

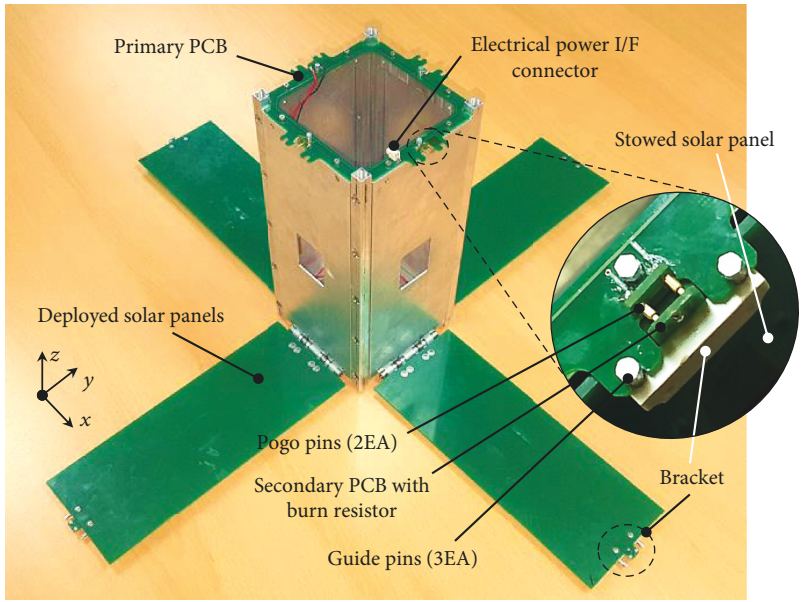

Figure 4: Demonstration model of the pogo pin-type holding and release mechanism.

The mechanism mainly consists of a PCB, guide pins, burn resistors, spring-loaded pogo pins, and brackets. The basic operation principle for holding and releasing a mechanical constraint is based on the burn wire release method, and this is extensively used for CubeSat applications. The mechanical constraint force on the deployable solar panel is applied by nylon cable tightening and triangular guide pins installed on the bracket and rail structure of the CubeSat. The two guide pins on the bracket mounted on the solar panel also provide a mechanical interface to implement a mechanical constraint along the in-plane direction of the solar panel, and this is achieved by a combination with the U-shaped interface on the main PCB. The mechanical constraints on both the in-plane and the out-of-plane directions of the solar panel are extremely advantageous for the mechanism that differentiates it from the conventional mechanism, based on the burn wire release method. The release of the nylon cable winding along the guide pins is initiated by the activation of burn resistors soldered on the secondary PCB mounted on the bracket, as shown in Figure 4. The secondary PCB with a burn resistor is integrated on the bracket at a distance that slightly exceeds the position of the two guide pins such that tensioning is applied on the wire attached to the resistor during the tightening process of the nylon cable. This guarantees a significantly more reliable cut through the nylon wires. The rear side of the secondary PCB includes an electrical interface to provide power to the burn resistor on the front side of the PCB. The spring-loaded pogo pins are considered in the design to establish a temporary electrical connection between the two PCBs before the initiation of the release action. The provision of power to the resistor from the primary PCB is achieved through the pogo pins. The PCB dedicated for the installation of pogo pins is vertically integrated to the primary PCB through a soldering process, as shown in Figure 4. Additionally, the power connector used to distribute power to each pogo pin interface is also

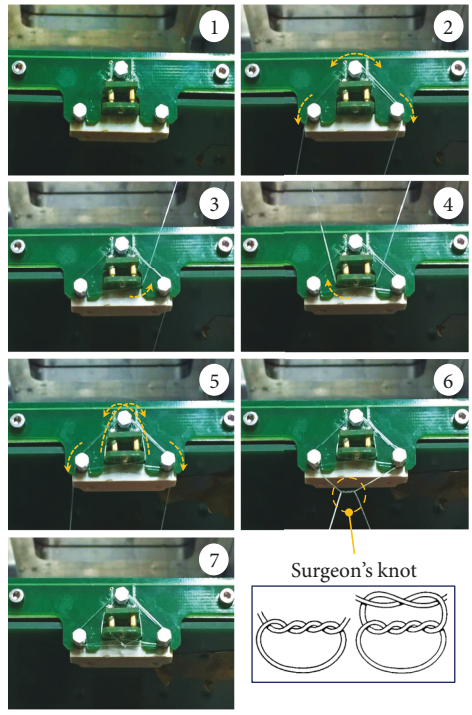

Figure 5: An optimized tightening process of the nylon cable demonstrated along three guide pins of the mechanism.

positioned on the primary PCB for the synchronous release of multiple panels. An extremely important feature of the pogo pin mechanism is that it is used as a status switch to determine a deployment status of the solar panel although it primarily functions as an electrical interface to provide power to the resistor. Additionally, a pogo pin is also used as a separation spring to initiate a reaction force to the stowed solar panel. The spring force from the pogo pin is useful to

Table 1: Specifications of the spring-loaded pogo pin, nylon cable, and burn resistor.

Item	Details	Value
Spring-loaded pogo pin	Manufacturer	Hanbit T&I Co.
	Maximum allowable voltage and current	12 V, 2.0 A
	Contact resistance	Max. 30 mΩ
	Maximum number of loadings	30,000
	Qualification temperature	−40°C–85°C
	Operation power of spring-loaded pin	0.78 N ± 0.16 N
Nylon wire	Manufacturer	Toray Co.
	Material	Fluorocarbon
	Diameter	0.2 mm
	Maximum allowable force	57.88 N
Burn resistor	Manufacturer	Walsin Technology Co.
	Package	Surface mount device (SMD)
	Package size code	3216
	Electrical resistance	4.7 Ω
	Resistance tolerance	±1%
	Max. power dissipation	0.25 W (T_{amb} = 70°C)

perform a reliable cut through the nylon cable because the tensioning is continually applied to the cable by the restoration force of the compressed pogo pin.

Figure 5 shows an optimized tightening process of the nylon cable along three guide pins applied in the mechanism. The process is validated through a function test of the mechanism and guarantees an increased tightening force and reliable release of the mechanical constraint on the cables. The handling simplicity of the tightening process of the nylon wire is an extremely important advantage of the mechanism because the knotting process is considerably simpler and reliable when compared to the conventional method.

Table 1 lists the specifications of the pogo pin used in the demonstration model of the mechanism shown in Figure 4. The table also summarizes the specifications of the nylon cable and burn resistor used in the model. The pogo pin exhibits the maximum allowable voltage and current corresponding to 12 V and 2.0 A, respectively. Its qualified temperature ranges from −40°C to 85°C. The maximum allowable number of loadings applied to the pogo pin is 30,000. With respect to the tightening of the solar panels, we used a fluorocarbon cable with a diameter of 0.2 mm and a maximum allowable force of 57.88 N. Additionally, a surface mount device (SMD) chip resistor type with a resistance value of 4.7 Ω was used as the burn resistor. Table 2 summarizes the mass budget of the demonstration model of the mechanism shown in Figure 4. The total mass of the mechanism system is 18.4 g.

Table 2: Mass budget of the demonstration model of the mechanism.

Item	Mass (g)
Primary PCB	12.8
Secondary PCB with burn resistor (4EA)	1
Brackets (4EA)	2.8
Guide pins (12EA)	1.8
Total	18.4

3. Validation Test Results

Figure 6 shows the functional test configuration of the mechanism used to validate a stable release function and measure the natural frequency of the stowed solar panel. The demonstration model of the pogo pin-type HRM mechanism is integrated in the 2 U dummy CubeSat structure with four PCBs simulating the solar panels, as shown in Figure 6. In order to measure the dynamic response from the solar panel after synchronous burn wire triggering, accelerometers with a thickness of 1.5 mm were attached on each dummy PCB solar panel. An infrared (IR) camera (FLIR T-420) was used to monitor the temperature increase in the thermal resistor during input voltage triggering to the pogo pins. In the test, the input voltage and current to the pogo pins were measured to determine the deployment status of the mechanism. This was employed to verify whether it was possible to use the pogo pins as a status switch. A power supply was used to provide the input voltage to the pogo pins. Release function tests were performed three times under various test conditions, including differences in the number of cable windings, temperature conditions, and input voltages.

Figure 7 shows sequential images captured by the high-speed camera of a successful release of the HRM with pogo pins at ambient temperature conditions. The images indicate that the synchronous release of dummy solar panels is successful without any interference induced by the mechanism. The time from the triggering of the burn wire to the release is approximately 6.2 s when the input voltage and ambient temperature correspond to 5 V and 20°C, respectively.

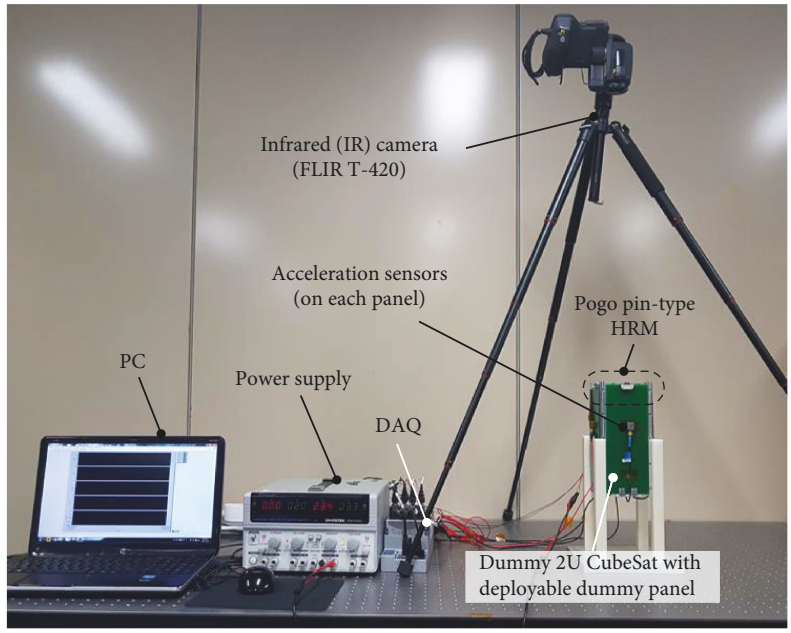

Figure 6: Test setup for a release function test of the demonstration model of the pogo pin-type holding and release mechanism.

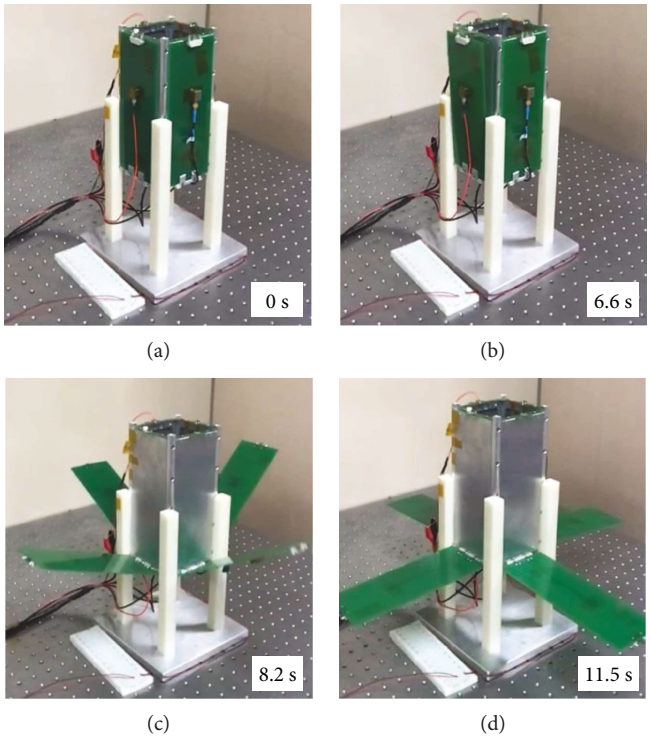

Figure 7: Example of a successful release sequence of the mechanism.

Figure 8 shows the temperature images captured by the IR camera during the release activation of the HRM. The result indicates that the mechanical constraint on the nylon wire is released when the temperature in the resistor increases to approximately 104°C and that 6.1 s elapse from the ambient temperature of 20°C. The temperature increases in the four resistors after triggering exhibit almost identical behaviors and guarantee a synchronous release of multiple panels.

Figure 9 shows the time histories for the acceleration of each panel, input voltage, and current, measured on the pogo pins during the release function test with an input voltage of 5 V. The release time after the application of the triggering input voltage was approximately equal to 6.2 s, and the acceleration data measured on the dummy panels indicate that the maximum time gap between the released panels is 0.56 s. The voltage and current measured on the pogo pins indicate step signals after the release of the electrical contact between the primary and second PCBs. This is because the four sets of pogo pins are connected in parallel with the use of the electrical power interface connector. This fact indicates that it is possible to use the pogo as a status switch in accordance to the proposed mechanism design.

Figure 10 shows the release times of the solar panels when the input voltages of 5 V and 8 V are applied. In the test, a mechanical constraint with one cable winding is implemented on the proposed mechanism, and three release function tests are performed under ambient room temperature. The mechanism exhibited successful release in all the tested cases, and the release time was reduced to 1.4 s by increasing the input voltage to 8 V, as provided by a Li-ion battery [16] with a maximum capacity of 2600 mAh for CubeSat applications. The response time was reduced under vacuum because it is reported that the burn release mechanism exhibits a faster response under vacuum when compared to that in air [18]. Additionally, the test results indicated that the mechanism also provided a synchronous release of multiple panels because the gap of the release time for each panel in each test case was within 0.5 s.

Figure 11 shows the release time of each solar panel with various numbers of cable windings when the input voltage to the mechanism was set to 8 V. The results indicate that the

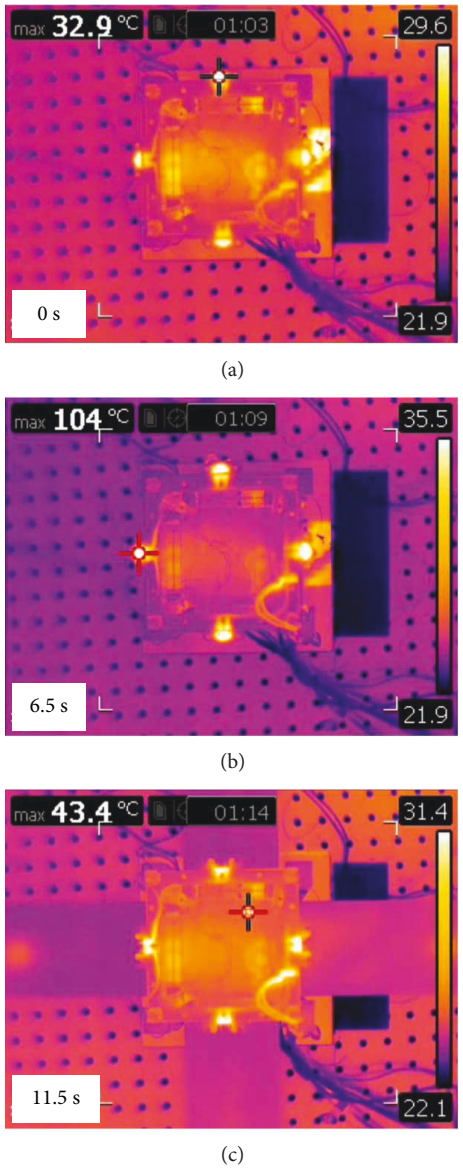

Figure 8: IR image taken at the maximum temperature of the burn resistor of the mechanism.

release time increases when the number of cable windings increases. The mechanism with the triple cable windings shows a release time that is less than 2.2 s and guarantees a synchronous release of the multiple solar panels.

Figure 12 shows the normalized natural frequencies of the solar panel for different numbers of cable windings for a relative comparison. The absolute frequency value is meaningless as dummy solar panels with a thickness of 1.5 mm are used for the test. The y-axis in the figure denotes the ratio of $f_{\text{cable}}/f_{\text{rigid}}$, where f_{rigid} and f_{cable} denote the measured natural frequencies of the solar panel when the panel is rigidly fixed and clamped by nylon cables, respectively. The measured value of f_{rigid} for the dummy PCB panel with a thickness of 1.5 mm that consisted of FR4 is 78.7 Hz. The ratio of $f_{\text{cable}}/f_{\text{rigid}}$ increases when the number of cable windings increases.

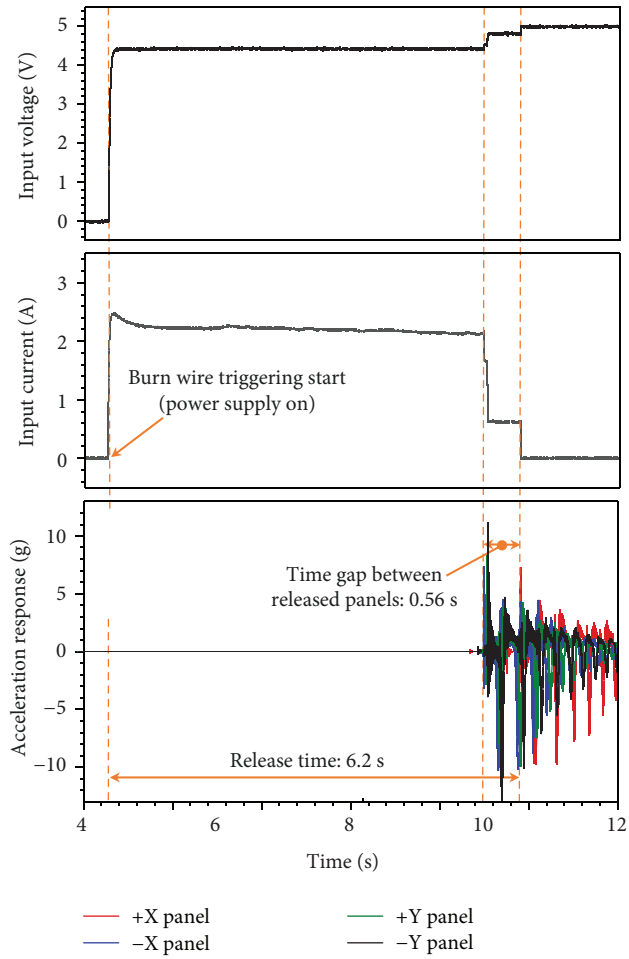

Figure 9: Time profiles of the input voltage and current of the mechanism and acceleration responses of the solar panels.

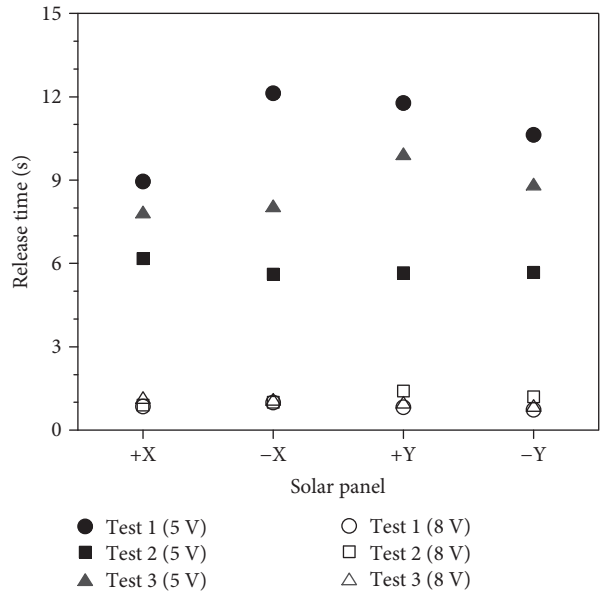

Figure 10: Release time of each solar panel when the input voltages of 5 V and 8 V are applied on the mechanism.

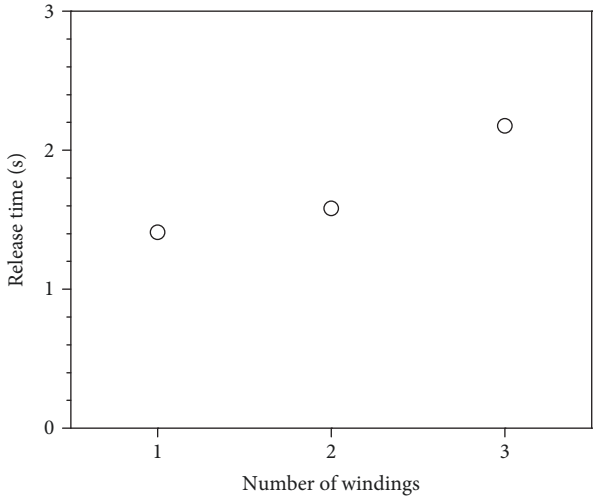

Figure 11: Release times of each solar panel as a function of the number of cable windings for an input voltage of 8 V.

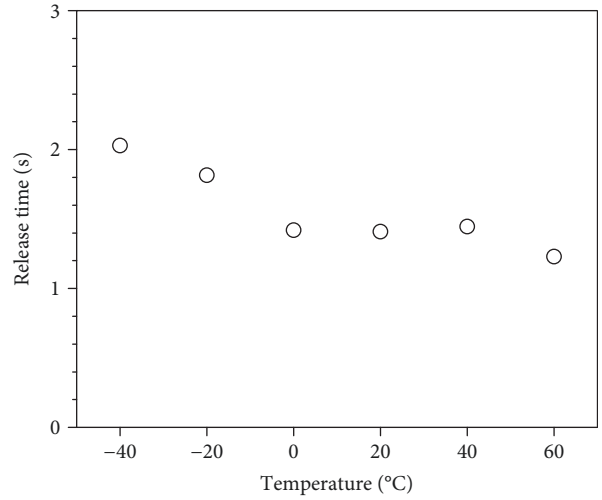

Figure 13: Release time of each solar panel as a function of qualification temperature ranges at an input voltage of 8 V.

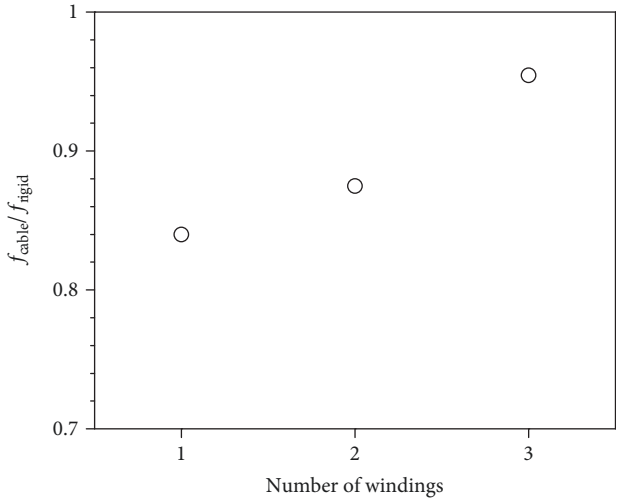

Figure 12: Normalized natural frequency of the solar panel for different numbers of cable windings.

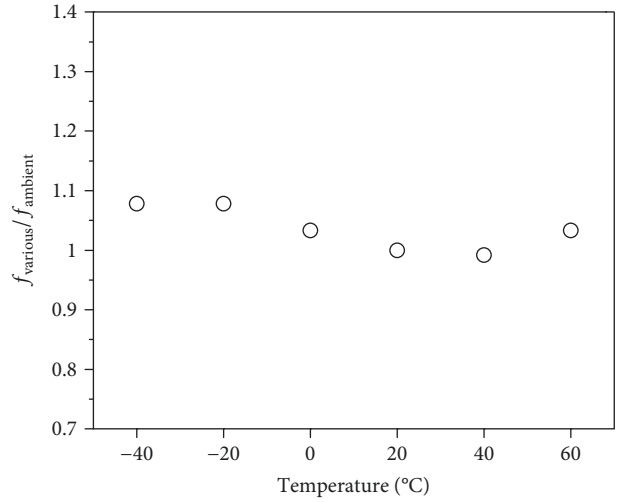

Figure 14: Normalized natural frequency of the solar panel as a function of qualification temperature ranges.

To confirm the functional performance of the mechanism under the qualification temperature limits of −40°C and 70°C, we performed functional tests with the same test configuration, as shown in Figure 6. In the experiment, the temperature reference point used to determine the stabilized target temperature is located near the pogo pin interface of the primary PCB. The results are obtained when the input voltage to the mechanism is set to 8 V in the case where single cable winding was used. As shown in Figure 13, the measured release times were less than 2.26 s and 1.25 s under low- and high-temperature conditions, respectively. The test results indicate that the mechanism functioned well below the low-temperature limits.

Figure 14 shows the normalized natural frequency of the solar panel as a function of qualification temperature ranges. The y-axis in the figure denotes the ratio $f_{various}/f_{ambient}$, where $f_{ambient}$ and $f_{various}$ denote the measured natural frequencies of the solar panel of an ambient temperature of 20°C and various qualification temperature ranges, respectively. The results indicate that the frequency of the mechanism with respect to the temperature variation was negligibly low under the temperature ranges from −40°C to 70°C.

In this study, we performed additional validation tests of the proposed mechanism by using a Dyneema wire with a higher strength and a lower outgassing and ultraviolet (UV) resistance, compared with the nylon wire. In addition, the wire had a space heritage [24]. The test setup was the same as that shown in Figure 6. The Dyneema wire used in this study had a thickness of 0.12 mm, a maximum allowable strength of 67.95 N, and a melting point of 80°C. The release time and acceleration responses of dummy panels were

obtained using single cable winding when the input voltage was 8 V. The results indicated that the release time after triggering of input voltage was approximately within 2.46 s, and the time gap between released panels was 0.43 s. In addition, the results of repetitive separation tests indicated that the variation of release time was no more than 0.5 s. These results indicated that the mechanism proposed in this study also ensures a stable function by using the Dyneema wire for tightening the solar panels.

In the case of the pogo pin HRM proposed in this study, the accessibility was considerably improved as most of the parts were installed on the external side of the CubeSat. Therefore, an inspection and a reworking of the parts, such as secondary PCB or pogo pins, can be performed without removing the solar panel. In addition, the tightening process of the nylon wire shown in Figure 5 guarantees the reset capability of the mechanism for reliable holding and release of solar panels. These capabilities are expected to be highly advantageous, especially in the acceptance test process of the flight model of the CubeSat.

4. Conclusion

In the study, we proposed and investigated the use of a spring-loaded pogo pin as a holding and release mechanism of solar panels for cube satellite applications. The pogo pin is advantageous for applications of separation devices because it functions as an electrical interface, a separation spring, and a status switch. The proposed mechanism in the study that involves the use of the pogo pin includes increased loading capability along the in-plane and out-of-plane directions of the solar panels, negligible shock levels, synchronous release of multiple panels, and handling simplicity during the tightening process of the nylon wire. In addition, the ability for inspection and reworking of the mechanism parts owing to the improved accessibility is highly advantageous, especially in the acceptance test process of the CubeSat. The feasibility of the proposed mechanism for CubeSat applications was demonstrated through the separation tests using test conditions that included various input voltages, different numbers of tightened nylon wires, and different temperatures (ranging from −40°C to 70°C). A future study will validate the structural safety and functionality of the mechanism in an on-orbit environment based on a launch vibration test and a thermal vacuum cycling test at a qualification level.

Data Availability

The data used to support the findings of this study are available from the corresponding author upon request.

Conflicts of Interest

The authors declare that there is no conflict of interest regarding the publication of this manuscript.

References

[1] K. Woellert, P. Ehrenfreund, A. J. Ricco, and H. Hertzfeld, "Cubesats: cost-effective science and technology platforms for emerging and developing nations," *Advances in Space Research*, vol. 47, no. 4, pp. 663–684, 2011.

[2] P. Ehrenfreund, A. J. Ricco, D. Squires et al., "The O/OREOS mission—astrobiology in low Earth orbit," *Acta Astronautica*, vol. 93, pp. 501–508, 2014.

[3] V. Lappas, N. Adeli, L. Visagie et al., "CubeSail: a low cost CubeSat based solar sail demonstration mission," *Advances in Space Research*, vol. 48, no. 11, pp. 1890–1901, 2011.

[4] M. Tsay, J. Frongillo, K. Hohman, and B. K. Malphrus, "LunarCube: a deep space 6U CubeSat with mission enabling ion propulsion technology," in *29th Annual AIAA/USU Conference on Small Satellites, SSC15-XI-1*, pp. 1–8, Logan, UT, USA, 2015.

[5] E. Gill, P. Sundaramoorthy, J. Bouwmeester, B. Zandbergen, and R. Reinhard, "Formation flying within a constellation of nano-satellites: the QB50 mission," *Acta Astronautica*, vol. 82, no. 1, pp. 110–117, 2013.

[6] J. A. Vilán Vilán, F. Aguado Agelet, M. López Estévez, and A. González Muiño, "Flight results: reliability and lifetime of the polymeric 3D-printed antenna deployment mechanism installed on Xatcobeo & Humsat-D," *Acta Astronautica*, vol. 107, pp. 290–300, 2015.

[7] X. Li, Q. Schiller, L. Blum et al., "First results from CSSWE CubeSat: characteristics of relativistic electrons in the near-earth environment during the October 2012 magnetic storms," *Journal of Geophysical Research: Space Physics*, vol. 118, no. 10, pp. 6489–6499, 2013.

[8] S. H. Youn, Y. S. Jang, and J. H. Han, "Compressed mesh washer isolators using the pseudoelasticity of SMA for pyroshock attenuation," *Journal of Intelligent Material Systems and Structures*, vol. 21, no. 4, pp. 407–421, 2010.

[9] http://www.tiniaerospace.com.

[10] http://www.dynalloy.com/.

[11] H. U. Oh, M. S. Jo, K. M. Lee, and D. J. Kim, "Spaceborne tilt mirror mechanism and application of shape memory alloy actuator to implement fail-safe function in emergency mode," *Transactions of the Japan Society for Aeronautical and Space Sciences*, vol. 55, no. 6, pp. 373–378, 2012.

[12] B. Saggin, D. Scaccabarozzi, M. Tarbini, M. Magni, C. A. Biffi, and A. Tuissi, "Design of a smart bidirectional actuator for space operation," *Smart Materials and Structures*, vol. 26, no. 3, article 035041, 2017.

[13] D. J. Hartl and D. C. Lagoudas, "Aerospace applications of shape memory alloys," *Proceedings of the Institution of Mechanical Engineers, Part G: Journal of Aerospace Engineering*, vol. 221, no. 4, pp. 535–552, 2007.

[14] K. Nakaya, K. Konoue, H. Sawada et al., "Tokyo Tech CubeSat: CUTE-I-design & development of flight model and future plan," in *21st International Communications Satellite Systems Conference and Exhibit*, pp. 2003–2388, Yokohama, Japan, 2003.

[15] A. Thurn, S. Huynh, S. Koss et al., "A nichrome burn wire release mechanism for CubeSats," in *The 41st Aerospace Mechanisms Symposium, Jet Propulsion Laboratory*, pp. 479–488, Pasadena, CA, USA, May 2012.

[16] http://www.gomspace.com.

[17] H. U. Oh and M. J. Lee, "Development of a non-explosive segmented nut-type holding and release mechanism for cube

satellite applications," *Transactions of the Japan Society for Aeronautical and Space Sciences*, vol. 58, no. 1, pp. 1–6, 2015.

[18] M. J. Lee, Y. K. Lee, and H. U. Oh, "Performance evaluation of hinge driving separation nut-type holding and releasing mechanism triggered by nichrome burn wire," *International Journal of Aeronautical and Space Sciences*, vol. 16, no. 4, pp. 602–613, 2015.

[19] S. J. Kang and H. U. Oh, "On-orbit thermal design and validation of 1 U standardized CubeSat of STEP cube lab," *International Journal of Aerospace Engineering*, vol. 2016, Article ID 4213189, 17 pages, 2016.

[20] Y. Temiz, R. D. Lovchik, G. V. Kaigala, and E. Delamarche, "Lab-on-a-chip devices: how to close and plug the lab?," *Microelectronic Engineering*, vol. 132, pp. 156–175, 2015.

[21] https://www.mill-max.com/new_products/detail/103.

[22] B. B. Szendrenyi, H. Barnes, J. Moreira, M. Wollitzer, T. Schmid, and M. Tsai, "Addressing the broadband crosstalk challenges of pogo pin type interfaces for high-density high-speed digital applications," in *2007 IEEE/MTT-S International Microwave Symposium*, pp. 2209–2212, Honolulu, HI, USA, June 2007.

[23] H. U. Oh, T. G. Kim, S. H. Han, and J. K. Lee, "Verification of MEMS fabrication process for the application of MEMS solid propellant thruster arrays in space through launch and on-orbit environment tests," *Acta Astronautica*, vol. 131, pp. 28–35, 2017.

[24] http://www.dsm.com/products/dyneema/en_GB/home.html.